

Mini-Proceedings, 16th meeting of the Working Group on Radiative Corrections and MC Generators for Low Energies

18th - 19th November, Laboratori Nazionali di Frascati, Italy

Editors

Henryk Czyz (Katowice), Pere Masjuan (Mainz), Graziano Venanzoni (Frascati)

ABSTRACT

The mini-proceedings of the 16th Meeting of the "Working Group on Radiative Corrections and MonteCarlo Generators for Low Energies" held in Frascati, 18th - 19th November, are presented. These meetings, started in 2006, have as aim to bring together experimentalists and theoreticians working in the fields of meson transition form factors, hadronic contributions to the anomalous magnetic moment of the leptons, and the effective fine structure constant. The development of MonteCarlo generators and Radiative Corrections for precision e^+e^- and τ -lepton physics are also covered.

The web page of the conference:

<https://agenda.infn.it/conferenceDisplay.py?ovw=True&confId=8626>

contains the presentations.

We acknowledge the support and hospitality of the Laboratori Nazionali di Frascati.

Contents

1	Introduction to the Workshop	3
	<i>H. Czyż and G. Venanzoni</i>	
2	Summaries of the talks	5
2.1	Present accuracy and future prospects of Monte Carlo generators for Bhabha and $e^+e^- \rightarrow \gamma\gamma$	5
	<i>C.M. Carloni</i>	
2.2	Current status of luminosity measurement with the CMD-3 detector at the VEPP-2000 e^+e^- collider	8
	<i>G.V.Fedotov</i>	
2.3	The role of experimental data as input information for precise hadronic calculations: muon $g - 2$, rare π^0 decays, and mixing parameters	11
	<i>P. Masjuan</i>	
2.4	On the positronium contribution to the electron $g - 2$	14
	<i>M. Passera</i>	
2.5	Hadronic light-by-light scattering in the muon $g - 2$: a dispersive approach .	16
	<i>M. Hoferichter</i>	
2.6	Primary Monte-Carlo generator of the process $e^+e^- \rightarrow a_0(980)\rho(770)$ for the CMD-3 experiment	19
	<i>P.A. Lukin</i>	
2.7	Automation of the leading order calculations for $e^+e^- \rightarrow$ hadrons	21
	<i>K. Kolodziej</i>	
2.8	MCGPJ for the processes $e^+e^- \rightarrow$ hadrons for experiments with CMD-3 detector at the VEPP-2000 collider	24
	<i>G.V. Fedotov</i>	
2.9	χ_{c1} and χ_{c2} production at e^+e^- colliders - preliminary results	28
	<i>S. Tracz</i>	
2.10	Nucleon form factors in PHOKHARA	30
	<i>H. Czyż</i>	
2.11	Current status of Monte Carlo generator Tauola	32
	<i>O. Shekhovtsova</i>	
3	List of participants	34

1 Introduction to the Workshop

H. Czyż¹ and G. Venanzoni²

¹Institute of Physics, University of Silesia, 40007 Katowice, Poland

²Laboratori Nazionali di Frascati dell'INFN, 00044 Frascati, Italy

The importance of continuous and close collaboration between the experimental and theoretical groups is crucial in the quest for precision in hadronic physics. This is the reason why the Working Group on “Radiative Corrections and Monte Carlo Generators for Low Energies” (Radio MonteCarLow) was formed a few years ago bringing together experts (theorists and experimentalists) working in the field of low-energy e^+e^- physics and partly also the τ community. Its main motivation was to understand the status and the precision of the Monte Carlo generators used to analyze the hadronic cross section measurements obtained as well with energy scans as with radiative return, to determine luminosities, and whatever possible to perform tuned comparisons, *i.e.* comparisons of MC generators with a common set of input parameters and experimental cuts. This main effort was summarized in a report published in 2010 [1]. During the years the WG structure has been enriched of more physics items and now it includes seven subgroups: Luminosity, R-measurement, ISR, Hadronic VP $g - 2$ and Delta alpha, gamma-gamma physics, FSR models, tau.

During the workshop the last achievements of each subgroups have been presented. The present accuracy and the future prospects of MC generators for e^+e^- into leptonic, $\gamma\gamma$, and hadronic final states have been reviewed. The recent evaluation of the positronium contribution to the electron $g - 2$ and the role of experimental data to the hadronic LO and Light-by-Light NLO contributions to the $g - 2$ of the muon have been discussed. New results from CMD3 and BESIII experiments have been presented. Finally the status of HPrecisionNet work package of the networking program HPH to Horizon 2020, was presented.

The workshop was held from the 18th to the 19th November, at the Laboratori Nazionali di Frascati dell'INFN, Italy.

Webpage of the conference is

<https://agenda.infn.it/conferenceDisplay.py?ovw=True&confId=8626>

where detailed program and talks can be found.

All the information on the WG can be found at the web page:

<http://www.lnf.infn.it/wg/sighad/>

References

- [1] S. Actis *et al.* [Working Group on Radiative Corrections and Monte Carlo Generators for Low Energies Collaboration], Eur. Phys. J. C **66** (2010) 585 [arXiv:0912.0749 [hep-ph]].
- [2] P. Masjuan, G. Venanzoni, H. Czyż, A. Denig, M. Vanderhaeghen, G. Venanzoni, A. Denig and S. Eidelman *et al.*, arXiv:1306.2045 [hep-ph].

- [3] H. Czyż, S. Eidelman, G. V. Fedotov, A. Korobov, S. E. Mller, A. Nyffeler, P. Roig and O. Shekhovtsova *et al.*, arXiv:1312.0454 [hep-ph].
- [4] J. J. van der Bij, H. Czyż, S. Eidelman, G. Fedotov, T. Ferber, V. Ivanov, A. Korobov and Z. Liu *et al.*, arXiv:1406.4639 [hep-ph].

2 Summaries of the talks

2.1 Present accuracy and future prospects of Monte Carlo generators for Bhabha and $e^+e^- \rightarrow \gamma\gamma$

C.M. Carloni Calame

Dipartimento di Fisica, Università di Pavia, Via A. Bassi 6, 27100 Pavia, Italy

The knowledge of the luminosity \mathcal{L} is a key ingredient for any measurement at e^+e^- machines. The usual strategy to calculate it is through the relation $\mathcal{L} = N/\sigma_{th}$, where σ_{th} is the theoretical cross section of a QED process and N the number of events. QED processes are the best choice because of their clean signal, low background and the possibility to push the theoretical accuracy up to the 0.1% level or better. The latter requires the inclusion of the relevant radiative corrections (RCs) and their implementation into Monte Carlo (MC) event generators (EGs) to easily account for experimental event selection criteria.

Modern EGs used for luminometry simulate Bhabha, $e^+e^- \rightarrow \gamma\gamma$ and $e^+e^- \rightarrow \mu^+\mu^-$ (or a sub-set of them), including the exact NLO QED corrections and/or a leading-log (LL) approximation of higher-order (h.o.) effects [1, 2, 3, 4, 5]. The consistent inclusion of NLO and h.o. LL contributions is mandatory in view of the required theoretical accuracy.

Focusing on Bhabha scattering, in order to estimate the theoretical error of the EGs, it is extremely important to perform tuned comparisons among them, to assess the technical precision and have an idea of the accuracy of the included corrections, usually implemented according to different approaches. This has been done and reported in [6], from which tab. 1 has been extracted. In general, it is found that the different MC EGs predict cross sections

setup	BabaYaga@NLO	BHWIDE	MCGPJ	$\delta(\%)$
$\sqrt{s} = 1.02 \text{ GeV}, 20^\circ \leq \vartheta_{\mp} \leq 160^\circ$	6086.6(1)	6086.3(2)	—	0.005
$\sqrt{s} = 1.02 \text{ GeV}, 55^\circ \leq \vartheta_{\mp} \leq 125^\circ$	455.85(1)	455.73(1)	—	0.030
$\sqrt{s} = 3.5 \text{ GeV}, \vartheta_+ + \vartheta_- - \pi \leq 0.25 \text{ rad}$	35.20(2)	—	35.181(5)	0.050
$\sqrt{s} = 10 \text{ GeV}, 40^\circ \leq \vartheta_{\mp} \leq 160^\circ$	11.67(3)	11.660(8)	—	0.086

Table 1: Comparison of Bhabha cross sections (in nb) for different setups, obtained with the EGs described in [1], [2] and [3]. See [6] for further details and results.

which differ by at most 0.1% when including NLO and h.o. LL corrections. This is in fair agreement with the accuracy of the different approaches estimated by the authors.

A further step to put on firmer ground the theoretical error is to compare with exact NNLO results, which have been calculated for Bhabha scattering by various groups in the last years (see references in [6]). NNLO RCs are partly included in EGs and, once extracted, their NNLO contributions can be consistently compared with exact calculations. This has been done for example in the 3rd paper of [1] and in [7].

In Tab. 2 (adapted from [6]) the total error “budget” is summarized for typical luminometry conditions at flavor factories. The main conclusion to draw from it is that RCs currently implemented into MC EGs allow to reach a theoretical precision up to the 0.1% level.

Source of error (%)	Φ –factories	$\sqrt{s} = 3.5$ GeV	B –factories
$ \delta_{\text{VP}}^{\text{err}} $	0.02	0.01	0.02
$ \delta_{\text{SV},\alpha^2}^{\text{err}} $	0.02	0.02	0.02
$ \delta_{\text{HH},\alpha^2}^{\text{err}} $	0.00	0.00	0.00
$ \delta_{\text{SV,H},\alpha^2}^{\text{err}} $	0.05	0.05	0.05
$ \delta_{\text{pairs}}^{\text{err}} $	0.03	0.016	0.03
$ \delta_{\text{total}}^{\text{err}} $ linearly	0.12	0.1	0.13
$ \delta_{\text{total}}^{\text{err}} $ in quadrature	0.07	0.06	0.06

Table 2: Total error “budget” for Bhabha cross section at flavor factories. See [1, 6, 7] for more details and definitions.

It has to be mentioned that the error induced by vacuum polarization (VP) corrections is driven and dominated by experimental errors. At energies around the narrow resonances (such as J/Ψ), VP errors might be larger than in tab. 2 and a dedicated study is needed.

A similar picture ought to be valid also for $\gamma\gamma$ final state, with the added advantage that, at least up to NLO, VP corrections do not contribute to the cross section. Nevertheless, a careful estimate of the theoretical error in this case has not been performed yet and would be of high interest.

A possible improvement of the theoretical accuracy, if going beyond the 0.1% level is needed at all, would be the inclusion of the full NNLO results into the MC EGs, which is a non trivial but feasible task.

I’d like to thank H. Czyz and G. Venanzoni for the kind invitation and the organization of a really stimulating workshop.

References

- [1] C. M. Carloni Calame *et al.*, Nucl. Phys. B **584** (2000) 459 [hep-ph/0003268]
C. M. Carloni Calame *et al.*, Nucl. Phys. Proc. Suppl. **131** (2004) 48 [hep-ph/0312014]
G. Balossini *et al.*, Nucl. Phys. B **758** (2006) 227 [hep-ph/0607181]
G. Balossini *et al.*, Phys. Lett. B **663** (2008) 209 [arXiv:0801.3360 [hep-ph]]
- [2] S. Jadach, W. Placzek, B. F. L. Ward, Phys. Lett. B **390** (1997) 298 [hep-ph/9608412]
- [3] A. B. Arbuzov *et al.*, Eur. Phys. J. C **46** (2006) 689 [hep-ph/0504233]
- [4] E. Drago, G. Venanzoni, INFN-AE-97-48 (1997)
- [5] F. A. Berends, R. Kleiss, Nucl. Phys. B **228** (1983) 537
F. A. Berends, R. Kleiss, Nucl. Phys. B **186**, 22 (1981)

- [6] S. Actis *et al.*, Eur. Phys. J. C **66** (2010) 585 [arXiv:0912.0749 [hep-ph]].
- [7] C. M. Carloni Calame *et al.*, JHEP **1107** (2011) 126 [arXiv:1106.3178 [hep-ph]].

2.2 Current status of luminosity measurement with the CMD-3 detector at the VEPP-2000 e^+e^- collider

G.V.Fedotov^{1,2}, A.E.Ryzhenkov^{1,2}

¹Budker Institute of Nuclear Physics, SB RAS, Novosibirsk, 630090, Russia

²Novosibirsk State University, Novosibirsk, 630090, Russia

Since December 2010 the CMD-3 [1] detector has taken data at the electron-positron collider VEPP-2000 [2]. The collected data sample corresponds to an integrated luminosity of 60 pb^{-1} in the c.m. energy from 0.32 up to 2 GeV.

The luminosity is a key part in many experiments which study the hadronic cross sections at e^+e^- colliders. As a rule, the systematic error of the luminosity determination represents one of the largest sources of uncertainty which can cause significant reduction of the hadronic cross sections accuracy. Therefore it is very important to have several well known QED processes such as $e^+e^- \rightarrow e^+e^-$, $\mu^+\mu^-$, $\gamma\gamma$ to determine the luminosity. The combined application of them will help to better understand and estimate a real systematic accuracy of the luminosity. The combined application of them will help to better understand and estimate a real systematic accuracy of the luminosity.

The energy range from 1 to 2 GeV was scanned up and down with a step of 50 MeV. At each energy point the integrated luminosity $\sim 500 \text{ nb}^{-1}$ was collected. During the scan down the energy points, at which the data were collected, have been shifted to the previous one by 25 MeV. The data were collected at an average luminosity $\sim 4 \cdot 10^{30} \text{ s}^{-1} \cdot \text{cm}^{-2}$. At the highest energies the peak luminosity reached the values about $2 \cdot 10^{31} \text{ s}^{-1} \cdot \text{cm}^{-2}$ and was restricted by the positron storage rate in the booster. The project luminosity $\sim 10^{32} \text{ s}^{-1} \cdot \text{cm}^{-2}$ will be provided only with start of operating of new positron injection facility in 2015. The beam energy has been monitored ($\sim 0.5 \text{ MeV}$) by measuring the current in dipole magnets of the main ring. The time period of this run was extend from January to June 2011. In 2012 the luminosity was measured at 16 energy points from 1.32 GeV to 1.98 GeV and collected luminosity was about $\sim 14 \text{ pb}^{-1}$.

In 2013 the energy range from 0.32 GeV to 1 GeV was scan with the 10 MeV step. The integrated luminosities about 8.3 and 8.4 pb^{-1} were collected around ω and ϕ mesons. Over the 2013 year the integrated luminosity $\sim 25 \text{ pb}^{-1}$ has been collected.

The sample of collinear events e^+e^- , $\mu^+\mu^-$, $\pi^+\pi^-$, K^+K^- and cosmic background were selected for luminosity determination. The two-dimensional plot of energy deposition in calorimeters for these events is presented in Fig.1 for the beam energy 950 MeV. It is clear seen that Bhabha events are distributed predominantly at the upper right corner whereas other particles are concentrated in the bottom left one. Thus, the integrated luminosity can be determined by the well selected Bhabha events.

To select $\gamma\gamma$ events the information about they energy deposition in calorimeters is used. It is seen that the signal events are concentrated as a cluster of dots in upper-right corner of this plot. At the same time two train seen - concentration of dots in two mutually perpendicular directions due to ISR. The events of this sample should have energy deposition inside interval: $0.5E_{beam} < E_0, E_1 < 1.5E_{beam}$. Unfortunately the small part of the Bhabha

events can seep under the central peak and imitate $\gamma\gamma$ events. To exclude such events the additional condition was applied - the Z-chamber sectors associated with clusters must be triggered. Visual scan of the remaining events proofed - there are not Bhabha events under central. Unfortunately this condition delete some $\gamma\gamma$ events due to albedo coming from showers. The fraction of such events amounts to $\sim 6\%$ and as a result we should include correction about 0.36% to restore the number of $\gamma\gamma$ events.

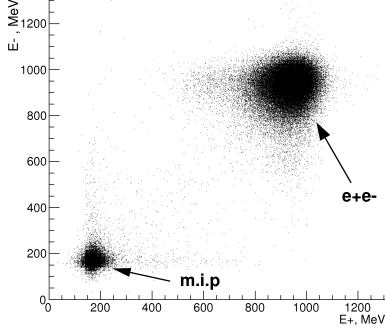


Figure 1: Two-dimensional plot of energy deposition in calorimeters one particle vs another for collinear tracks.

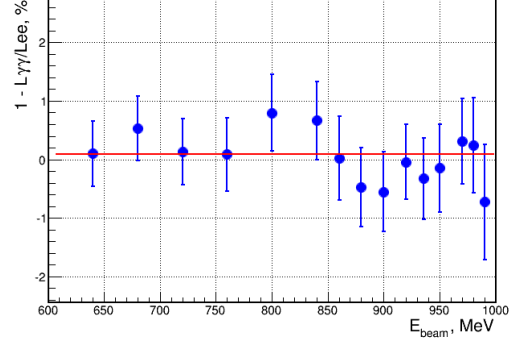


Figure 2: The ratio of the luminosities for the e^+e^- and $\gamma\gamma$ processes vs energy. Scan 2012. The horizontal red line - fit.

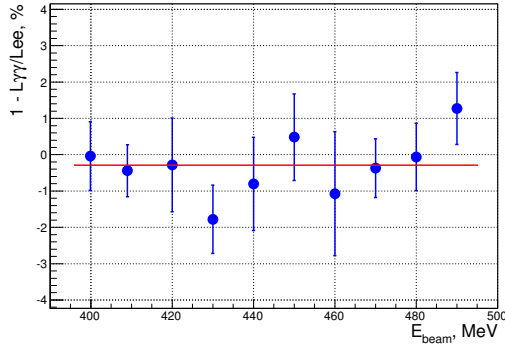


Figure 3: The ratio of the luminosities for the e^+e^- and $\gamma\gamma$ processes vs energy. Scan 2013. The horizontal red line - fit.

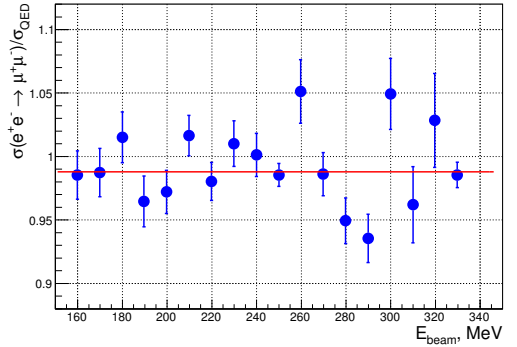


Figure 4: The results of cross section measurement of muon production in comparison with the prediction of QED.

The luminosities ratio determined with use of two processes vs energy is presented in Fig. 2 and in Fig. 3, where only statistical errors are shown. The blue circles correspond to the scan up, whereas red circles - scan down. The horizontal line is a fit for this ratio for scan down. In this case the relative difference between luminosities is in average $(0.73 \pm 0.35)\%$. However, at the beginning of the run the difference was $\sim 3\%$ and explained by hardware problems and the quality of inter-calibration of the detector subsystems. Collecting all the

main sources which contribute to systematic error of the luminosity, we estimate the current accuracy as $\sim 1\%$ while. The first energy scan below 1 GeV was performed at VEPP-2000 during the season of 2013. The preliminary results of the luminosity measurement are shown in Fig. 3. The already collected statistics is higher than that in the previous CMD-2 experiment and at the level or better than in BaBar and KLOE experiments. One of the tests in this analysis is to measure the cross section of the process $e^+e^- \rightarrow \mu^+\mu^-$ at low energy, where particles separation is possible using only momentum information from DC. Preliminary results of this test are consistent with the QED prediction as it is seen in Fig. 4. The radiative corrections (RC) to this cross section with photon jets radiation in collinear regions were taken into account according to [5] and their accuracy is better than 0.2%.

References

- [1] B.I.Khazin *et al.*, Nucl.Phys.B, Proc. Suppl. **181-182**, 376 (2008).
- [2] V.V. Danilov *et al.*, Proceedings of EPAC96, Barcelona, p.1593 (1996).
I.A. Koop, Nucl. Phys. B (Proc. Suppl.) **181-182**, 371 (2008).
- [3] G.Grawford *et al.*, NIM **A345**, 429 (1994).
- [4] A.Arbuzov *et al.*, EPJ **C46**, 689 (2006).
- [5] S.Actis *et al.*, Eur. Phys. J. **C66**, 585 (2010).

2.3 The role of experimental data as input information for precise hadronic calculations: muon $g - 2$, rare π^0 decays, and mixing parameters

P. Masjuan

PRISMA Cluster of Excellence, Institut für Kernphysik, Johannes Gutenberg-Universität, Mainz D-55099, Germany

One of the open questions concerning the Hadronic Light-by-Light scattering contribution to the muon $g - 2$ (HLBL) is the role of experimental data.

Part of the difficulty of including experimental data in the HLBL is due to the particular framework where the main calculations are done [1], the large- N_c of QCD [2]. In such limit, one uses the resonance saturation scheme to reproduce the pseudoscalar transition form factor (TFF) that appears in the dominant piece of the HLBL, the pseudoscalar-exchange contribution [1]. The main inputs are, then, the pion decay constant and the values of the resonance masses. On top, even though data on the TFF are willing to be included, one still faces the problem on how to link the different kinematic regimes between the experiment for the TFF (low-energy region at time- and space-like, together with intermediate energies at space like) and the kinematics for the pseudoscalar-exchange diagram (whole space-like energy region, from origin of energies up to infinity) [1].

In this talk I summarized our attempt to provide an answer to that question in a model-independent fashion [3]¹, a method based on the analyticity of the TFF, compatible with the recent dispersion relations approach [5] with the advantage of having larger photon energy range of applicability (in practice, the full energy range), and based on the low-energy properties of the TFF. This endeavor started two years ago in Ref. [6] and was further developed in Refs. [3, 4, 7].

The method proposed can be summarized as follows:

- our attempt is, indeed, a method, not *a model*.
- it shall be simple, easy to understand, to apply and reproduce, in contrast to more involved procedures such as dispersion relations.
- it may contain approaches (to say, improvable), but not assumptions (not improvable).
- it should be systematic, easy to update with new experimental data but also it should provide a systematic error, a pure error from the method itself.
- finally, it should be predictive meaning checkable

The method proposed is based on the mathematical theory of Padé approximants (PA). It was pointed out in Ref. [8] that, in the large- N_c framework, the resonance saturation scheme employed in the HLBL can be understood from the theory of PA to meromorphic

¹For a recent summary, see for instance Ref. [4]

functions [9], where one can compute the desired quantities in a model-independent way. Also, the analytical properties of the TFF indicate that the convergence of the PA is guaranteed at the energies we are working with. Altogether defines the systematics of our method (more iterations should give better approximation) and ascribe an error to that [10].

To exemplify the advantages of our method, we considered a model from Ref. [11]. As stated before, the inputs for the model can have two different sources: first, a pure theoretical origin based on large- N_c and chiral limits (inputs are resonance masses within the *half-width rule* [12] and the meson decay constant in the chiral $SU(3)$ limit [13]); second, a reconstruction of the models based on a matching with the TFF low-energy constants [6], i.e, *à la* PA [8, 9, 10] minimizing in such a way the model dependence (see [4] for details). The former yields a final error for the π^0 contribution to HLBL to 15% (5% from F_0 and 10% from the masses). The later, the Padé method, yield a similar 15% provided that the 13% error on the slope (25% on curvature) implies an error of 10% (5%) in the pion contribution; the impact of F_π is dramatic since its 1% error implies a 2% error on HLBL. Interestingly enough, the central value is 20% higher, driving non compatible results! The PA method, predictable [14], can accommodate space- and time-like data. Provides also a rule-of-thumb for estimating the impact of experimental uncertainties, a point never discussed before.

Notice, nevertheless, that the standard procedure [1, 11] to treat the TFF is through a factorization approach, e.g., $F(Q_1^2, Q_2^2) = F(Q_1^2, 0) \times F(0, Q_2^2)$ where $F(Q^2, 0)$ is the measured quantity. The impact of such approach is not negligible (see my contribution in [15]).

In conclusion, we remark the important role of experimental data to determine the dominant pieces of the HLBL (i.e., π^0, η, η'). We argue that the way of including such information should be based on PA which provides a systematic error and a simple rule for estimating the impact of experimental uncertainties, both from the space- and the time-like [3]. We notice, finally, that the errors discussed above have been unfortunately ignored in the main reviews (no error for F_0 or resonance masses have been properly estimated, neither the possibility to match with experimental low-energy description of the TFF) and that poses a warrant on the reliability of the current error estimates for the HLBL. Similar discussions concerning $P \rightarrow l^+l^-$ as well as mixing angles were also addressed.

As discussed during the meeting, to extract resonance poles using PA, see Ref.[16].

References

- [1] F. Jegerlehner and A. Nyffeler, Phys. Rept. **477**, 1 (2009) [arXiv:0902.3360 [hep-ph]].
- [2] G. 't Hooft, Nucl. Phys. B **72**, 461 (1974).
- [3] P. Masjuan and P. Sanchez-Puertas, *In preparation*.
- [4] P. Masjuan, arXiv:1411.6397 [hep-ph].
- [5] See M. Hoferichter in this proceedings.
- [6] P. Masjuan, Phys. Rev. D **86**, 094021 (2012) [arXiv:1206.2549 [hep-ph]]; P. Masjuan and M. Vanderhaeghen, arXiv:1212.0357 [hep-ph].
- [7] R. Escribano, P. Masjuan and P. Sanchez-Puertas, Phys. Rev. D **89** (2014) 3, 034014 [arXiv:1307.2061 [hep-ph]].

- [8] P. Masjuan and S. Peris, JHEP **0705**, 040 (2007) [arXiv:0704.1247 [hep-ph]]; Phys. Lett. B **663**, 61 (2008) [arXiv:0801.3558 [hep-ph]].
- [9] G. A. Baker and P. Graves-Morris, Encyclopedia of Mathematics and its Applications, Cambridge Univ. Press, 1996; P. Masjuan Queral, arXiv:1005.5683 [hep-ph].
- [10] P. Masjuan, *et al.*, Phys. Lett. B **668** (2008) 14 [arXiv:0805.3291 [hep-ph]]; P. Masjuan and S. Peris, Phys. Lett. B **686**, 307 (2010) [arXiv:0903.0294 [hep-ph]].
- [11] M. Knecht and A. Nyffeler, Phys. Rev. D **65**, 073034 (2002) [hep-ph/0111058].
- [12] P. Masjuan, E. Ruiz Arriola and W. Broniowski, Phys. Rev. D **85**, 094006 (2012) [arXiv:1203.4782 [hep-ph]]; Phys. Rev. D **87**, 014005 (2013) [arXiv:1210.0760 [hep-ph]]; Phys. Rev. D **87** (2013) 11, 118502 [arXiv:1305.3493 [hep-ph]].
- [13] G. Ecker, *et al.*, Eur. Phys. J. C **74** (2014) 2748 [arXiv:1310.8452 [hep-ph]].
- [14] P. Aguar-Bartolome *et al.* [A2 Collaboration], Phys. Rev. C **89** (2014) 4, 044608 [arXiv:1309.5648 [hep-ex]].
- [15] P. Adlarson *et al.*, arXiv:1412.5451 [nucl-ex].
- [16] P. Masjuan *et al.*, Eur. Phys. J. C **73** (2013) 2594 [arXiv:1306.6308 [hep-ph]]; Phys. Rev. D **90** (2014) 9, 097901 [arXiv:1410.2397 [hep-ph]].

2.4 On the positronium contribution to the electron $g - 2$

M. Fael¹ and M. Passera²

¹ Albert Einstein Center for Fundamental Physics, Institute for Theoretical Physics, University of Bern, CH-3012 Bern, Switzerland

² Istituto Nazionale Fisica Nucleare, Sezione di Padova, I-35131 Padova, Italy

The leading contribution of positronium, the e^+e^- bound state, to the anomalous magnetic moment of the electron (a_e) has been computed in Ref. [1]. The result of this calculation,

$$a_e^{\text{P}} = \frac{\alpha^5}{4\pi} \zeta(3) \left(8 \ln 2 - \frac{11}{2} \right) = 0.89 \times 10^{-13}, \quad (1)$$

where $\zeta(3) = 1.202\dots$ and α is the fine-structure constant, is of the same order of α as the perturbative QED five-loop contribution $a_e^{(10)} = 9.16(58)(\alpha/\pi)^5$ [2] and comparable with the present experimental uncertainty $\delta a_e = 2.8 \times 10^{-13}$ [3]. As it seems reasonable to expect a reduction of δa_e to a part in 10^{-13} (or better) in ongoing efforts to improve this measurement, and work is in progress to reduce the error induced in the theoretical prediction for a_e by the uncertainty of α [4, 5], a test of the electron $g-2$ at the level of 10^{-13} (or below) is a goal that may be achieved not too far in the future. This will bring a_e to play a pivotal role in probing new physics and allow to test whether the long-standing $3-4\sigma$ discrepancy in the muon $g-2$ also manifests itself in the electron one [6].

Recently the authors of Ref. [7] pointed out the presence of the continuum nonperturbative contribution

$$a_e(\text{vp})^{\text{cont,np}} = -\frac{|\alpha|^5}{8\pi} \zeta(3) \left(8 \ln 2 - \frac{11}{2} \right) \quad (2)$$

arising from the region right above the $s = 4m^2$ threshold, which corresponds to e^+e^- scattering states with the exchange of Coulomb photons. Comparing Eqs. (1) and (2) they showed that this additional $\mathcal{O}(\alpha^5)$ nonperturbative contribution cancels one-half of that of the positronium poles. The question is therefore how to deal with the remaining half: should one add it to the perturbative five-loop QED result of Ref. [2]? Reference [7] argued that this remaining $a_e^{\text{P}}/2$ term is already contained in the perturbative $\mathcal{O}(\alpha^5)$ contribution to a_e computed in Ref. [2] and, therefore, it should not be added to it. On the other hand, in Ref. [8] it was claimed that positronium contributes to a_e only through diagrams of $\mathcal{O}(\alpha^7)$ or higher. Also, on more general grounds [9], Ref. [10] argued that a_e^{P} does not exist.

In order to clarify this issue, in Ref. [11] we used the closed form for the QED vacuum polarization function near the $s = 4m^2$ threshold of Refs. [9, 12] to verify that the total (positronium poles plus continuum) nonperturbative contribution to a_e arising from the threshold region is equal to $a_e^{\text{P}}/2$. Then, using the analytic QED vacuum polarization at four-loop of Ref. [13], we showed explicitly that the perturbative five-loop calculation of a_e of Ref. [2] does indeed contain the remaining term $a_e^{\text{P}}/2$, in agreement with the arguments of Ref. [7]. We also showed that this term $a_e^{\text{P}}/2$ arises from the class I(i) of five-loop diagrams of Ref. [14] containing only one closed electron loop.

In conclusion, we showed explicitly that there is no additional contribution of QED bound states to a_e beyond perturbation theory.

Acknowledgments The work of M.F. is supported by the Swiss National Science Foundation. M.P. thanks the Department of Physics and Astronomy of the University of Padova for its support. His work was supported in part by the PRIN 2010-11 of the Italian MIUR and by the European Program INVISIBLES (PITN-GA-2011-289442).

References

- [1] G. Mishima, arXiv:1311.7109 [hep-ph].
- [2] T. Aoyama, M. Hayakawa, T. Kinoshita and M. Nio, Phys. Rev. Lett. **109** (2012) 111807 [arXiv:1205.5368 [hep-ph]].
- [3] D. Hanneke, S. Fogwell and G. Gabrielse, Phys. Rev. Lett. **100** (2008) 120801.
- [4] R. Bouchendira *et al.*, Phys. Rev. Lett. **106** (2011) 080801.
- [5] F. Terranova, G. M. Tino, Phys. Rev. A **89** (2014) 052118 [arXiv:1312.2346 [hep-ex]].
- [6] G. F. Giudice, P. Paradisi and M. Passera, JHEP **1211** (2012) 113 [arXiv:1208.6583 [hep-ph]].
- [7] K. Melnikov, A. Vainshtein and M. Voloshin, Phys. Rev. D **90** (2014) 017301 [arXiv:1402.5690 [hep-ph]].
- [8] M. Hayakawa, arXiv:1403.0416 [hep-ph].
- [9] M. A. Braun, Zh. Eksp. Teor. Fiz. **54** (1968) 1220 [Sov. Phys. JETP. **27** (1968) 652].
- [10] M. I. Eides, Phys. Rev. D **90** (2014) 057301 [arXiv:1402.5860 [hep-ph]].
- [11] M. Fael and M. Passera, Phys. Rev. D **90** (2014) 056004 [arXiv:1402.1575 [hep-ph]].
- [12] R. Barbieri, P. Christillin and E. Remiddi, Phys. Rev. A **8** (1973) 5, 2266.
- [13] P. A. Baikov, A. Maier and P. Marquard, Nucl. Phys. B **877** (2013) 647 [arXiv:1307.6105 [hep-ph]].
- [14] T. Aoyama, M. Hayakawa, T. Kinoshita and M. Nio, Phys. Rev. D **83** (2011) 053003 [arXiv:1012.5569 [hep-ph]].

2.5 Hadronic light-by-light scattering in the muon $g - 2$: a dispersive approach

M. Hoferichter^{1,2}

¹ Institut für Kernphysik, Technische Universität Darmstadt, Germany

² ExtreMe Matter Institute EMMI, GSI Helmholtzzentrum für Schwerionenforschung GmbH, Germany

The uncertainty in the Standard-Model prediction for the anomalous magnetic moment of the muon is dominated by strong interactions. While hadronic vacuum polarization is intimately related to $e^+e^- \rightarrow$ hadrons by means of a dispersion integral, a similarly data-driven approach has only recently been suggested for hadronic light-by-light scattering (HLbL) (see [1, 2] for even higher-order hadronic contributions). Our framework [3, 4] exploits the analytic structure of the HLbL tensor, concentrating on pseudoscalar poles and two-meson intermediate states, which dominate at low energies.² The key input quantities for such a program are the doubly-virtual pion transition form factor [7] and the partial waves for $\gamma^*\gamma^* \rightarrow \pi\pi$ [8, 9, 10, 11, 12], which in the absence of doubly-virtual data can again be reconstructed dispersively (see [13] for a similar approach to the η, η' transition form factor).

The calculation of the pion transition form factor [7] can be understood as a generalization of existing analyses for $\gamma\pi \rightarrow \pi\pi$ [14] and $\omega, \phi \rightarrow 3\pi$ [15], which provide access to the form factor at fixed isoscalar virtualities $q_s^2 = 0$ and $q_s^2 = M_\omega^2, M_\phi^2$ [16], respectively. However, the normalization of the amplitude for a given q_s^2 cannot be predicted, but needs to be inferred from experiment, in case of $\gamma\pi \rightarrow \pi\pi$ by means of the Wess–Zumino–Witten anomaly, in case of $\omega, \phi \rightarrow 3\pi$ via the decay width. For general q_s^2 , the normalization is extracted from $e^+e^- \rightarrow 3\pi$ cross-section data, providing a prediction for $e^+e^- \rightarrow \pi^0\gamma$ without adjusting further parameters. So far, the phenomenological analysis of the singly-virtual form factor has been carried out, including accurate predictions for the slope of the form factor and its analytic continuation into the space-like region.

A crucial step in the derivation of our dispersive formalism [3] concerns the construction of a suitable basis for the HLbL tensor, in such a way that the coefficient functions are free of kinematic singularities [17, 18, 19]. Moreover, contributions involving double-spectral regions need to be considered separately, so that the sQED pion loop augmented with pion vector form factors (FsQED), as identified on the level of the Mandelstam representation, is evaluated based on Feynman loop integrals. In the talk, also a first numerical evaluation of S -wave $\pi\pi$ intermediate states was presented. Despite the double-spectral regions and solely based on S -waves the FsQED contribution can be reproduced at the (5–10)% level. Including $\pi\pi$ rescattering in the $\gamma^*\gamma^* \rightarrow \pi\pi$ partial waves in a simplified formalism that involves a Born-term left-hand cut and a finite matching point below the $K\bar{K}$ threshold, we find that the sum of $I = 0$ and $I = 2$ rescattering contributes $\sim -5 \times 10^{-11}$ and, taken

²A different approach, which aims at a dispersive description of the muon vertex function instead of the HLbL tensor, has recently been presented in [5]. An alternative strategy to reduce the model dependence in HLbL is based on lattice QCD [6].

together with FsQED, $\sim -20 \times 10^{-11}$ to HLbL scattering in the muon $g - 2$.

References

- [1] A. Kurz, T. Liu, P. Marquard and M. Steinhauser, Phys. Lett. B **734** (2014) 144 [arXiv:1403.6400 [hep-ph]].
- [2] G. Colangelo, M. Hoferichter, A. Nyffeler, M. Passera and P. Stoffer, Phys. Lett. B **735** (2014) 90 [arXiv:1403.7512 [hep-ph]].
- [3] G. Colangelo, M. Hoferichter, M. Procura and P. Stoffer, JHEP **1409** (2014) 091 [arXiv:1402.7081 [hep-ph]].
- [4] G. Colangelo, M. Hoferichter, B. Kubis, M. Procura and P. Stoffer, Phys. Lett. B **738** (2014) 6 [arXiv:1408.2517 [hep-ph]].
- [5] V. Pauk and M. Vanderhaeghen, arXiv:1409.0819 [hep-ph].
- [6] T. Blum, S. Chowdhury, M. Hayakawa and T. Izubuchi, arXiv:1407.2923 [hep-lat].
- [7] M. Hoferichter, B. Kubis, S. Leupold, F. Niecknig and S. P. Schneider, Eur. Phys. J. C **74** (2014) 3180 [arXiv:1410.4691 [hep-ph]].
- [8] R. García-Martín and B. Moussallam, Eur. Phys. J. C **70** (2010) 155 [arXiv:1006.5373 [hep-ph]].
- [9] M. Hoferichter, D. R. Phillips and C. Schat, Eur. Phys. J. C **71** (2011) 1743 [arXiv:1106.4147 [hep-ph]].
- [10] B. Moussallam, Eur. Phys. J. C **73** (2013) 2539 [arXiv:1305.3143 [hep-ph]].
- [11] M. Hoferichter, G. Colangelo, M. Procura and P. Stoffer, arXiv:1309.6877 [hep-ph].
- [12] L. Y. Dai and M. R. Pennington, Phys. Rev. D **90** (2014) 036004 [arXiv:1404.7524 [hep-ph]].
- [13] C. Hanhart, A. Kupść, U.-G. Meißner, F. Stollenwerk and A. Wirzba, Eur. Phys. J. C **73** (2013) 2668 [arXiv:1307.5654 [hep-ph]].
- [14] M. Hoferichter, B. Kubis and D. Sakkas, Phys. Rev. D **86** (2012) 116009 [arXiv:1210.6793 [hep-ph]].
- [15] F. Niecknig, B. Kubis and S. P. Schneider, Eur. Phys. J. C **72** (2012) 2014 [arXiv:1203.2501 [hep-ph]].
- [16] S. P. Schneider, B. Kubis and F. Niecknig, Phys. Rev. D **86** (2012) 054013 [arXiv:1206.3098 [hep-ph]].
- [17] W. A. Bardeen and W. K. Tung, Phys. Rev. **173** (1968) 1423 [Erratum-ibid. D **4** (1971) 3229].

- [18] R. Tarrach, Nuovo Cim. A **28** (1975) 409.
- [19] R. A. Leo, A. Minguzzi and G. Soliani, Nuovo Cim. A **30** (1975) 270.

2.6 Primary Monte-Carlo generator of the process $e^+e^- \rightarrow a_0(980)\rho(770)$ for the CMD-3 experiment

P.A. Lukin

Budker Institute of Nuclear Physics and Novosibirsk State University,
Russia, 630090, Novosibirsk

Electron-positron collider VEPP-2000 [1] has been operating in Budker Institute of Nuclear Physics since 2010. Center-of-mass energy ($E_{c.m.}$) range covered by the collider is from threshold of hadron production and up to 2 GeV. Special optics, so called “round beams”, used in the collider construction, allowed to obtain luminosity $2 \times 10^{31} \text{ cm}^{-2} \cdot \text{s}^{-1}$ at $E_{c.m.} = 1.8 \text{ GeV}$.

The general purpose detector CMD-3 has been described in detail elsewhere [2]. Its tracking system consists of a cylindrical drift chamber (DC) [3] and double-layer multiwire proportional Z-chamber, both also used for a trigger, and both inside a thin ($0.2 X_0$) superconducting solenoid with a field of 1.3 T. The liquid xenon (LXe) barrel calorimeter with $5.4 X_0$ thickness has fine electrode structure, providing 1-2 mm spatial resolution [4], and shares the cryostat vacuum volume with the superconducting solenoid. The barrel CsI crystal calorimeter with thickness of $8.1 X_0$ is placed outside the LXe calorimeter, and the end-cap BGO calorimeter with a thickness of $13.4 X_0$ is placed inside the solenoid [5]. The luminosity is measured using events of Bhabha scattering at large angles [6].

Physics program of the CMD-3 experiment includes the study of the multi-hadron production. The cross section measurement of the $e^+e^- \rightarrow 3(\pi^+\pi^-)$ process in $E_{c.m.} = 1.5 - 2.0 \text{ GeV}$ has been already published [7]. Preliminary results the study $2(\pi^+\pi^-\pi^0)$ final state has been reported [8].

The study of intermediate states which lead to $2(\pi^+\pi^-\pi^0)$ final state is essential to correctly describe the angular correlations between the particles and determine the registration efficiency of the process under study. As it was reported at [9] the intermediate states $\omega(782)3\pi$, $\omega(782)\eta(545)$ and $\rho(770)(4\pi)_{S\text{-}wave}$ allow satisfactorily describe mass and angular distributions of the $2(\pi^+\pi^-\pi^0)$ production in $E_{c.m.} = 1.5 - 1.7 \text{ GeV}$.

But for higher $E_{c.m.}$ it is not possible to describe $\eta(545)$ signal, seen in three-pion mass distribution of the $2(\pi^+\pi^-\pi^0)$, by contribution either $\omega(782)\eta(545)$ or $\phi(1020)\eta(545)$, because corresponding cross sections are small enough. We supposed that $\eta(545)$ can be explained by the process $e^+e^- \rightarrow a_0(980)\rho(770)$ with dominant decay of $a_0(980)$ into $\eta(545)\pi$. The primary Monte-Carlo generator for the process has been created out and implemented into the CMD-3 experiment Monte-Carlo simulation package. Using the generator the signal of the $e^+e^- \rightarrow a_0(980)\rho(770)$ process has been observed in the experimental data for $2(\pi^+\pi^-\pi^0)$ final state.

However, it was not possible to describe 2π - 3π and 4π mass distributions as well as angular correlations for $2(\pi^+\pi^-\pi^0)$ final state at $E_{c.m.} > 1.8 \text{ GeV}$ by contributions of $\omega(782)3\pi$, $a_0(980)\rho(770)$ and $\rho(770)4\pi$ intermediate states. Experimental 4π mass spectra demonstrate presence of narrow state. One of the candidate for this state is $f_0(1370)$ with dominant de-

cay into $\rho(770)\rho(770)$ and decays into $2(\pi^+\pi^-)$ and $\pi^+\pi^-2\pi^0$. So, the next step in the study of the $2(\pi^+\pi^-\pi^0)$ dynamics will be creation of the primary Monte-Carlo generator of the process $e^+e^- \rightarrow f_0(1370)(2\pi)_{P-wave}$.

References

- [1] V.V. Danilov *et al.*, Proceedings of EPAC96, Barcelona, p.1593 (1996).
I.A. Koop, Nucl. Phys. B (Proc. Suppl.) **181-182**, 371 (2008).
- [2] B.I. Khazin, Nucl. Phys. B (Proc. Suppl.) **181-182**, 376 (2008).
- [3] F. Grancagnolo *et al.*, Nucl. Instr. and Meth. A **623**, 114 (2010).
- [4] A.V. Anisyonkov *et al.*, Nucl. Instr. and Meth. A **598**, 266 (2009)
- [5] D. Epifanov (CMD-3 Collaboration), J. Phys. Conf. Ser. **293**, 012009 (2011).
- [6] R.R. Akhmetshin *et al.*, Nucl. Phys. B (Proc. Suppl.) **225-227**, 69 (2012).
- [7] R.R. Akhmetshin *et al.*, Phys.Lett. B**723** 82 (2013).
- [8] P.A. Lukin *et al.*, EPJ Web Conf. **81** 02010 (2014).
- [9] J.J. van der Bij *et al.*, arXiv:1406.4639 [hep-ph].

2.7 Automation of the leading order calculations for $e^+e^- \rightarrow$ hadrons

K. Kołodziej

Institute of Physics, University of Silesia, ul. Uniwersytecka 4, PL-40 007 Katowice, Poland

After some modifications, **carlomat** [1, 2], a program for automatic computation of the leading order (LO) cross sections of multiparticle reactions, that was originally dedicated mainly to description of the processes of production and decay of heavy particles such as top quarks, the Higgs boson, or electroweak gauge bosons, can be used to obtain predictions for $e^+e^- \rightarrow$ hadrons in the framework of effective models. At low energies, the hadronic final states consist mostly of pions, kaons, or nucleons which can be accompanied by one or more photons, or light fermion pairs such as e^+e^- , or $\mu^+\mu^-$. Some effective models which can be useful in this context, including the scalar electrodynamics (sQED) and the Wtb interaction with operators of dimension up to 5, were already implemented in version 2 of the program [2].

The effective Lagrangian of the Wtb interaction has the following form [3]:

$$L_{Wtb} = \frac{g}{\sqrt{2}} V_{tb} \left[W_\mu^- \bar{b} \gamma^\mu (f_1^L P_L + f_1^R P_R) t - \frac{1}{m_W} \partial_\nu W_\mu^- \bar{b} \sigma^{\mu\nu} (f_2^L P_L + f_2^R P_R) t \right] + \text{h.c.}, \quad (3)$$

where the couplings $f_i^L, f_i^R, i = 1, 2$, can be complex in general. The electromagnetic (EM) interaction of spin 1/2 nucleons has a similar form:

$$L_{\gamma NN} = e A_\mu \bar{N}(p') \left[\gamma^\mu F_1(Q^2) + \frac{i}{2m_N} \sigma^{\mu\nu} q_\nu F_2(Q^2) \right] N(p). \quad (4)$$

The form factors $F_1(Q^2)$ and $F_2(Q^2)$, where $Q^2 = -(p - p')^2$, were adopted from PHOKARA [4], thus making possible Monte Carlo (MC) simulations of processes involving the EM interaction of nucleons.

At low energies, π^\pm can be treated as point like particles and their EM interaction can be effectively described in the framework of sQED [5] the interaction vertices examples of which are shown in Fig. 5.

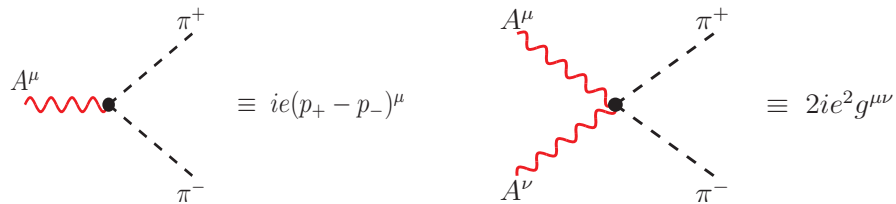


Figure 5: Vertices of sQED

Another step toward better description of $e^+e^- \rightarrow$ hadrons at low energies is the inclusion of the Feynman rules of the Resonance Chiral Perturbation Theory (RChPT). The

interaction vertices and particle mixing terms of RChPT that can be relevant in this context were provided by Fred Jegerlehner [6]. Some examples of them are shown in Figs. 6 and 7. The implementation of the triple and quartic interaction vertices was more or less straightforward, as it just required writing a few new subroutines for computation of the helicity amplitudes involving the Lorentz tensors that are different from those of the sQED vertices. The couplings $f_{\gamma PP}$, $f_{\rho^0 PP}$, $g_{\gamma\rho^0\pi\pi}$, $g_{\pi\gamma\gamma}$, $g_{\pi^0\gamma\rho^0}$ and $g_{\gamma\pi\pi\pi}$ are currently set either to 1 or e . However, implementation of the particle mixing is more challenging, because it must be added at the stage, where the topologies of diagrams which, in `carlomat`, contain only triple and quartic vertices, are confronted with the Feynman rules. This required substantial changes in the code generating part of the program.

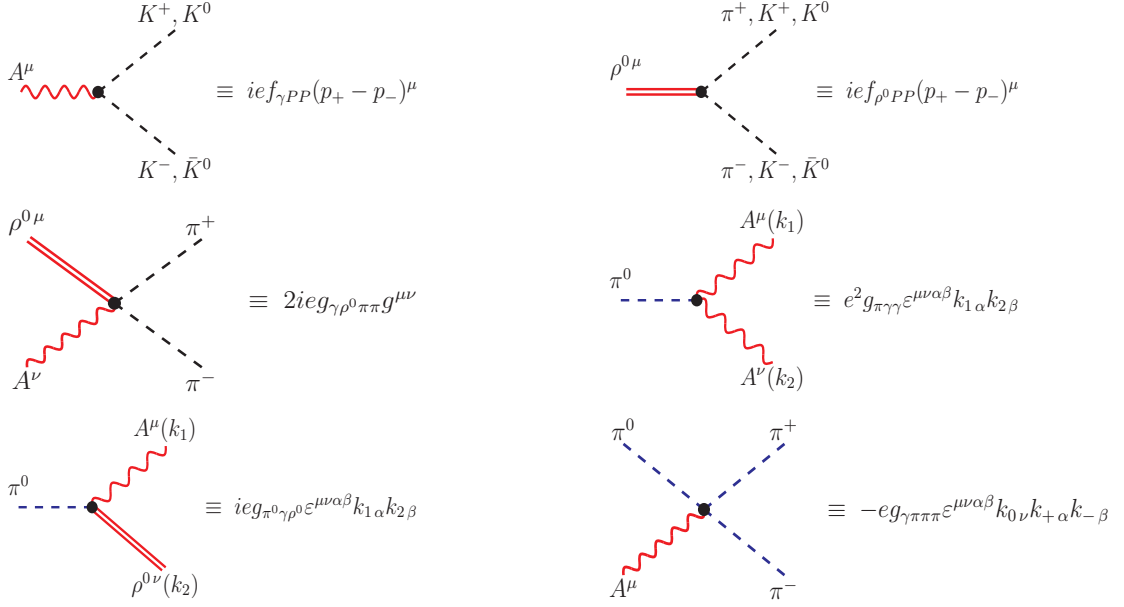


Figure 6: Examples of triple and quartic vertices of RChPT.

Figure 7 displays two Feynman diagrams representing particle mixing vertices. Each diagram is accompanied by its corresponding mathematical expression.

- Left:** A vertex with an incoming photon line (A^μ , wavy red) and an outgoing ρ^0 line ($\rho^{0\nu}$, double red). The expression is $\equiv -ef_{\gamma V}g^{\mu\nu}$.
- Right:** A vertex with an incoming W^\pm line ($W^{\pm\mu}$, wavy red) and an outgoing ρ^\mp line ($\rho^{\mp\nu}$, double red). The expression is $\equiv -ef_{W^\pm\rho^\mp}g^{\mu\nu}$.

Figure 7: Examples of the particle mixing.

To illustrate how the program works, consider the process $e^+e^- \rightarrow \pi^+\pi^-\pi^+\pi^-\gamma$. Taking into account the Feynman rules of the standard model and the rules of Figs. 5, 6 and 7, `carlomat` generates the $U(1)$ gauge invariant matrix element, which receives contributions from 903 LO Feynman diagrams, together with a dedicated multichannel phase space integration routine in just a few seconds. A computation of the total cross section, including any number of differential distributions, which is performed as the next step, takes several dozen seconds or several minutes time, dependent on the desired precision of the MC integration.

This project was supported in part with financial resources of the Polish National Science Centre (NCN) under grant decision No. DEC-2011/03/B/ST6/01615.

References

- [1] K. Kołodziej, Comput. Phys. Commun. **180** (2009) 1671, [arXiv:0903.3334].
- [2] K. Kołodziej, Comput. Phys. Commun. **185** (2014) 323, [arXiv:1305.5096].
- [3] G.L. Kane, G.A. Ladinsky, C.-P. Yuan, Phys. Rev. **D45** (1992) 124.
- [4] S. Tracz, H. Czyż, Acta Phys. Pol. **B44** (2013) 2281.
- [5] F. Jegerlehner, *The Anomalous Magnetic Moment of the Muon*, Springer, Nov. 2007, ISBN 9783540726333.
- [6] M. Benayoun, P. David, L. DelBuono, F. Jegerlehner, Eur. Phys. J. **C73** (2013) 2453.

2.8 MCGPJ for the processes $e^+e^- \rightarrow \text{hadrons}$ for experiments with CMD-3 detector at the VEPP-2000 collider

G.V. Fedotov, V.L. Ivanov, D.N. Shemyakin

Budker Institute of Nuclear Physics, SB RAS, Novosibirsk, 630090, Russia
Novosibirsk State University, Novosibirsk, 630090, Russia

The hadronic contribution to $(g-2)/2$ of muon, coming from VEPP-2000 energy range, is about 92%. One of the aims of the experiments with CMD-3 detector is to measure the main multihadrons cross sections (MHCS) with systematic uncertainty smaller than 3% (~ 0.15 ppm in $(g-2)/2$). The systematic accuracy of the cross section for the channel $e^+e^- \rightarrow \pi^+\pi^-$ at least better than 0.5% is required, as it is seen from the “bench” estimation. It is well known that the hadronic contribution to anomalous magnetic moment of muon (AMM) is about 60 ppm: $0.005 \times 60 \text{ ppm} = 0.3 \text{ ppm}$. The aim of the new FNAL and JPARC experiments to measure the $(g-2)/2$ of muon is to improve the previous BNL result by a factor of 4 and to achieve the accuracy of ~ 0.15 ppm - good test of the SM. It is obvious that the systematic uncertainty of radiative corrections (RC) for the MHCS should be smaller than 1 – 2%.

Previous experience of the studying of 3π channel at CMD-2 confirms, that final state radiation (FSR) contributes to the cross section (CS) at the level of 0.4% [1]. Obviously, that for the multihadron channels the contribution of FSR to CS will be smaller than 0.4%. In the scale of 1 – 2% for expected systematic accuracy we can neglect by FSR and consider photon jets radiation in collinear regions only. After many discussions with our experts in Dubna (JINR) we chose the following strategy, which will be described using the channels $e^+e^- \rightarrow K^+K^-\pi^+\pi^-$ and $e^+e^- \rightarrow K^+K^-\eta$ as the examples.

To select the clean signal events at first step four charged particles with zero net charge are selected using information from the drift chamber (DC). At the second step after the procedure of separation of kaons and pions (using dE/dx information [2]) we calculate the values: $\Delta E = E_1 + E_2 + E_3 + E_4 - 2E_{\text{beam}}$ and $|\vec{p}| = |\vec{p}_1 + \vec{p}_2 + \vec{p}_3 + \vec{p}_4|$. Two dimensional plot ΔE vs $|\vec{p}|$ for selected events is shown in Fig.1. The events of the signal process are inside the rectangle. The analysis of these events revealed that at least four intermediate states exist: $K^*\bar{K}^*$, $\phi\pi^+\pi^-$, $K^+K^-\rho$, $K^*(892)K\pi$. The simplest model was chosen to describe (more or less) correctly the experimental angular and momentum distributions. In Figures 2-5 the results of simulation vs experiment are presented. To increase the statistics we combine the data collected at several energy points. Red points correspond to experiment, black points - to simulation according to “realistic” model mentioned above, blue points - to simulation according to the $K^+K^-\pi^+\pi^-$ phase space. When the $K^+K^-\pi^+\pi^-$ events are selected and the dynamics of their production is defined we are able to calculate the detection efficiency and to determine the visible CS. In order to calculate the RC ($1 + \delta_{\text{rad}}(s)$) we calculate the following integral with Structure Functions $D(x, s)$ [3], which describe photon jets radiation in the collinear regions:

$$\sigma_{\text{vis}}(s) = \int_0^1 dx_1 \int_0^1 dx_2 D(x_1, s) D(x_2, s) \sigma_{\text{born}}(s(1-x_1)(1-x_2)) = (1 + \delta_{\text{rad}}(s)) \sigma_{\text{born}}(s).$$

At first iteration in the integral we use born CS, measured by BABAR (if there were not previous measurements of the born CS, then instead of the latter the visible CS should be used). This procedure is repeated for several iterations while RC does not become stable inside a corridor of $\sim 0.3\%$. The results of such calculation are plotted in Fig.6. The uncertainties of the RC are caused by the uncertainty of the form of the CS.

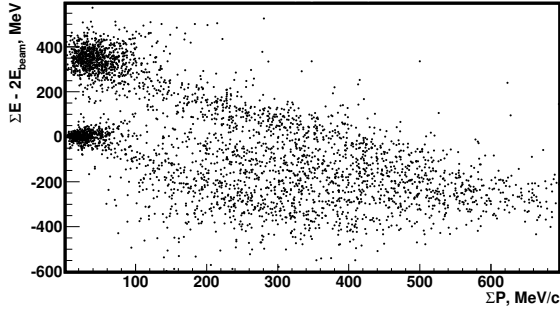


Figure 8: Two dimensional plot ΔE vs $|\vec{p}|$ for selected events. The $K^+K^-\pi^+\pi^-$ events are inside the rectangle.

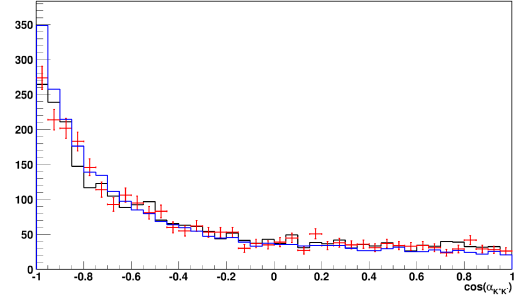


Figure 9: The distribution of the cosine of angle between K^+ and K^- .

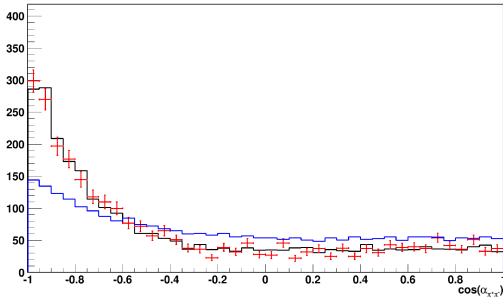


Figure 10: The distribution of the cosine of angle between π^+ and π^- .

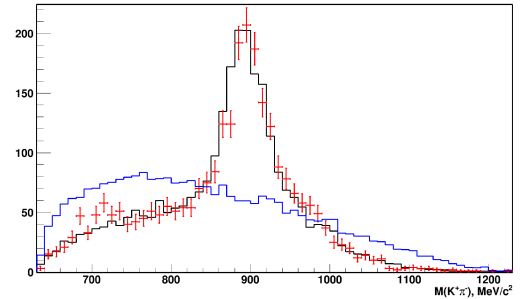


Figure 11: The distribution of the invariant mass of $K^-\pi^+$, $K^+\pi^-$.

This final state is almost completely produced by the $\phi(1680) \rightarrow \phi\eta$ mechanism. In our analysis we do not reconstruct the η from its decay products and do not use the information from calorimeters. This approach allows us to use all the modes of η decay and thus enlarges the statistics, but complicates background subtraction. The main sources of background here are $K^+K^-\pi^+\pi^-$ and $K^+K^-\pi^0\pi^0$ (especially their $\phi f_0(600)$ intermediate mechanism).

Using the information from DC we calculate the parameter $E_{\text{total}} - 2E_{\text{beam}}$:

$$E_{\text{total}} - 2E_{\text{beam}} = \sqrt{\vec{p}_{K^+}^2 + m_K^2} + \sqrt{\vec{p}_{K^-}^2 + m_K^2} + \sqrt{(-\vec{p}_{K^+} - \vec{p}_{K^-})^2 + m_\eta^2} - 2 \cdot E_{\text{beam}},$$

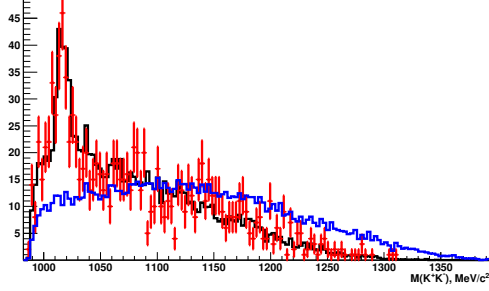


Figure 12: The distribution of the invariant mass of K^+K^- .

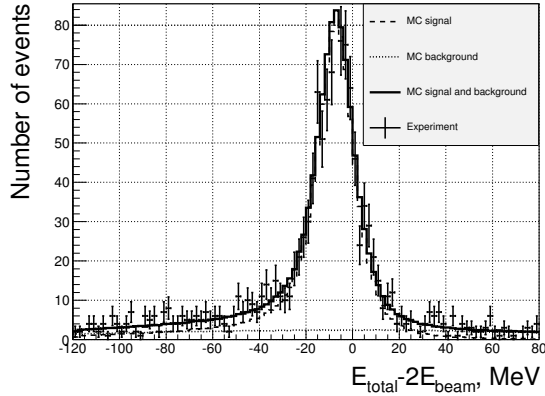


Figure 14: Results of separation of the signal and background: distribution of the parameter $E_{\text{total}} - 2E_{\text{beam}}$ (all energy points are combined) for 1) experiment (points with error bars) 2) signal events (open histogram with dashed line) 3) background events (open histogram with dotted line) 4) sum of signal and background events (open histogram with solid line).

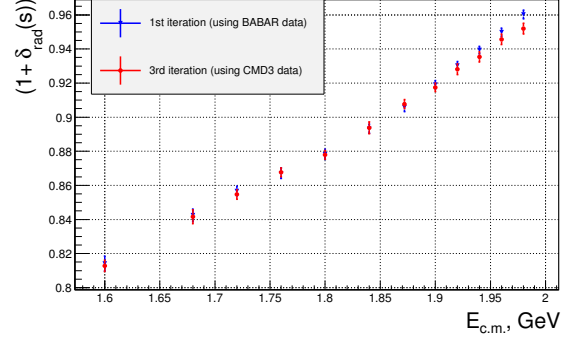


Figure 13: RC for $e^+e^- \rightarrow K^+K^-\pi^+\pi^-$: blue - 1st iteration on the base of BABAR born CS, red - 3rd iteration on the base of CMD-3 CS.

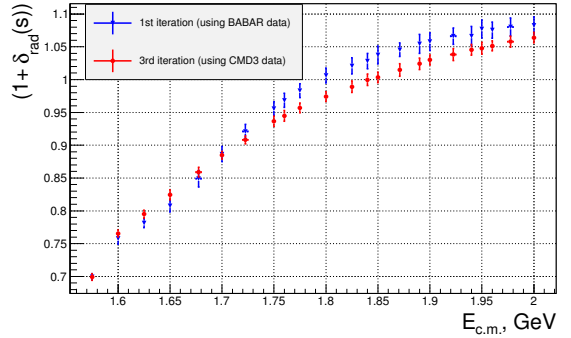


Figure 15: RC for $e^+e^- \rightarrow K^+K^-\eta$: blue - 1st iteration on the base of BABAR born CS, red - 3rd iteration on the base of CMD-3 CS.

which represents the total energy of the final particles minus twice beam energy in assumption that the missing particle is the η -meson. The distribution of this parameter for the $K^+K^-\eta$ has a peak around zero for any energy point and is used for defining the number of selected signal events $N_{K^+K^-\eta}^{\text{exp}}$. The shape of the distribution of this parameter for background is determined from MC. The results of the fitting of the experimental distributions are summarized in the Fig.7.

Having gotten the $N_{K^+K^-\eta}^{\text{exp}}$ and the detection efficiency we calculate the visible CS. The calculation of the RC is performed according the procedure, described above and shown in Fig.8.

In summary, we pointed out that until the precision of $\sim 1 - 2\%$ the multihadron cross sections can be studied without taking into account the FSR, i.e. considering photon jets radiation in collinear regions only. As the examples of such approach we have considered the calculation of RC for the processes $e^+e^- \rightarrow K^+K^-\pi^+\pi^-$ and $e^+e^- \rightarrow K^+K^-\eta$, which are under study at CMD-3.

References

- [1] A.B. Arbuzov (Dubna, JINR), G.V. Fedotovitch, F.V. Ignatov (Novosibirsk, IYF) *et al.* Eur.Phys.J. C46 (2006) 689-703
- [2] D.N. Shemyakin (Novosibirsk, IYF & Novosibirsk State U.), R.R. Akhmetshin, A. Anisenkov (Novosibirsk, IYF) *et al.* PoS Hadron2013 (2013) 138.
- [3] E.A. Kuraev, V.S. Fadin. Yad.Fiz. 41 (1985) 733-742.

2.9 χ_{c1} and χ_{c2} production at e^+e^- colliders - preliminary results

S. Tracz, H. Czyż, P. Kiszka

Institute of Physics, University of Silesia, Katowice, Poland

With the improving luminosity of e^+e^- colliders, the search for a production of 0^{++} , 1^{++} and 2^{++} states become possible. The production of these states goes through two virtual photons. The amplitude describing creation of the 0^{++} state through reaction $e^+e^- \rightarrow \chi_{c0}^* \rightarrow \dots$, going through loop diagram [1], is proportional to electron mass and thus highly suppressed. All χ_c states can be however produced through $e^+e^- \rightarrow e^+e^- \chi_{ci}^* (\rightarrow \dots)$, $i = 0, 1, 2$, reaction.

Measurements of the cross sections of the reaction $e^+e^- \rightarrow \chi_{c1,c2}^* \rightarrow \dots$ will allow to measure the electronic widths ($\Gamma_{e^+e^-}^{\chi_{c1,c2}}$) of the χ_{c1} and χ_{c2} resonances. Combined with measurements of the differential cross section of the reactions $e^+e^- \rightarrow e^+e^- \chi_{ci}^* (\rightarrow \dots)$ they will allow for detailed tests of models describing these charmonium bound states.

Expected range of $\Gamma_{e^+e^-}^{\chi_{c1,c2}}$ have been calculated inside two models, quarkonium model and vector dominance model already in [1]. Within the quarkonium model the amplitudes describing coupling of two virtual photons to J^{++} states depend on binding energy and the derivative of the wave function at the origin. This model predicts also that only some of the allowed amplitudes contribute. For χ_{c0} from two allowed amplitudes only one contributes. For χ_{c1} from three independent amplitudes one gives contribution. While for χ_{c2} from five possible amplitudes only one gives contribution.

For production of $\chi_{c0,1,2}$ states one can concentrate on a selected final state which is easy to be observed experimentally, mainly the decay of $\chi_{c0,1,2}$ into $J/\psi\gamma$, where J/ψ subsequently decays into pair of muons. For the $e^+e^- \rightarrow \chi_{c1,c2}^* \rightarrow J/\psi (\rightarrow \mu^+\mu^-) \gamma$ the process has to be considered together with radiative return process, which is a non-reducible background (see Figure 16 for diagrams). Furthermore one should take into account the unknown relative phase of the signal and the background amplitudes, which could give an interesting interference pattern. The binding energies and the derivative of the wave functions at the origin for $\chi_{c0,1,2}$ can be extracted from known [2] values of $\Gamma(\chi_{c0,1,2} \rightarrow \gamma\gamma)$ and $\Gamma(\chi_{c0,1,2,3} \rightarrow J/\psi\gamma)$. Assuming that the binding energies are different for each state and the derivative of the wave functions are equal, we have performed four fits. First fit was done to the data for χ_{c1} and χ_{c2} , second to the data for χ_{c0} and χ_{c1} , third to the data for χ_{c0} and χ_{c2} and fourth one to all data. The obtained results show that it is impossible to fit simultaneously the data for the states χ_{c0} and χ_{c2} . Thus the quarkonium model is not able to accommodate these data, even if the discrepancy is not dramatic. In the case of the global fit only width $\Gamma(\chi_{c0} \rightarrow \gamma\gamma)$ does not fit well. One has to remember however that the model is non-relativistic, while obtained binding energies and hence velocities of quarks are large. Using the fitted parameters we have made predictions of electronic widths. They are not greater than 0.1eV , which is at the limit of BES-III sensitivity.

To examine a possibility of studies of $\chi_c - \gamma^* - \gamma^*$ amplitudes at meson factories, we have calculated the cross section of the reaction $e^+e^- \rightarrow e^+e^- \chi_{ci}^* \rightarrow J/\psi (\rightarrow \mu^+\mu^-) \gamma$ within the same model. We have assumed integrated luminosities $L_{int} = 10\text{fb}^{-1}$ at energy 4.23

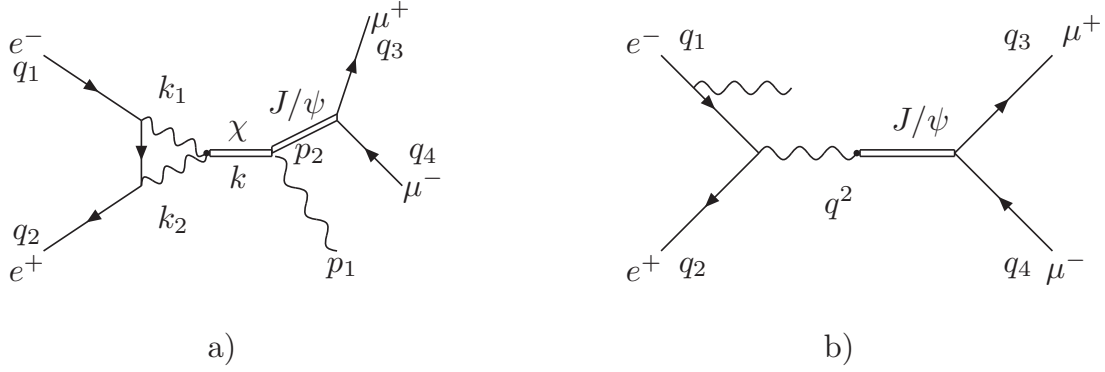


Figure 16: a) Diagram for process $e^+e^- \rightarrow \mu^+\mu^-$ with $\chi_{c1,2}$ production b) Diagram for radiative return process.

GeV(BES-III), $L_{int} = 530fb^{-1}$ (BaBar), $L_{int} = 1000fb^{-1}$ (BELLE) and $L_{int} = 50ab^{-1}$ (BELLE-2). In the last three we have used energy 10.56 GeV. For BES-III energy and luminosity the event rates are too small to be observed. The biggest expected rate is for χ_{c2} with 20 expected events if the final electron and positron are not tagged. For BaBar, BELLE and BELLE-2 the expected event rates with no electron-positron tagging are 1700, 3300, 160000 for χ_{c0} , 19000, 36000, 1800000 for χ_{c1} and 26000, 50000, 2500000 for χ_{c2} . For BELLE-2, even if one tags both electron and positron within the angular range $20^\circ - 160^\circ$, the expected event rates are big enough to be observed and are equal to 7500, 400000, 100000 for $\chi_{c0,c1,c2}$ respectively. The striking difference between $\chi_{c0,c2}$ and χ_{c1} seen here comes from the fact that for χ_{c1} the contribution from real photons is equal to zero and thus for small photons virtualities the amplitude is small.

The modes of production of $\chi_{c1,2}$ with the subsequent decay described above have been implemented in PHOKHARA Monte Carlo generator and the $\chi_{c0,c1,c2}$ production and decay mode was added in EKHARA Monte Carlo generator. Preliminary results shown above indicate that $\chi_{c0,1,2} - \gamma^* - \gamma^*$ amplitudes can be studied in existing or near future experiments. More detailed analysis will be presented in [3].

Work supported in part by the Polish National Science Centre, grant number DEC-2012/07/B/ST2/03867 and German Research Foundation DFG under Contract No. Collaborative Research Center CRC-1044. Szymon Tracz and Patrycja Kiswa are supported by the Forszt project co-financed by EU from the European Social Fund.

References

- [1] J. H. Kuhn, J. Kaplan and E. G. O. Safiani, Nucl. Phys. B **157** (1979) 125.
- [2] K. A. Olive *et al.* [Particle Data Group Collaboration], Chin. Phys. C **38** (2014) 090001.
- [3] H. Czyz, J. Kuhn, Sz. Tracz, P. Kiswa (in preparation)

2.10 Nucleon form factors in PHOKHARA

H. Czyż, S. Tracz

Institute of Physics, University of Silesia, PL-40007 Katowice, Poland

The electromagnetic nucleon form factors were studied from the conception of particle physics [1, 2, 3, 4]. and yet a lot has to be done to build a model which meets requirements in the era of precision hadronic physics. The not expected developments in this field show that we still have much to learn. The measurements of the ratio of the electric and magnetic form factors of the proton with two different methods were giving different results [5]. The two-photon exchange radiative corrections explaining to large extent this difference (see [6] for review) turned out to be unexpectedly large. Moreover their modelling goes beyond the nucleon form factor modelling adding to the complexity of the problem. In addition, usually the models are built separately in the space-like (see [7] for review) or time-like regions (see [8] for review). As one expects that each of the form factors is a unique analytic function valid in both space-like and time-like regions this attitude has to be changed and a model describing both regions has to be constructed. A step towards such a model was done in [9]. The model describes well data from both space-like and time-like regions. The form factors are normalised properly at zero invariant mass and, by construction, have correct behaviour [10] at large invariant masses. Yet the model is far from being satisfactory and further studies of photon-nucleon interactions are necessary. It is also clear that the progress can be achieved only through close collaboration of experimental and theory groups. Careful studies of charge and/or forward-backward asymmetries in $e^+e^- \rightarrow \bar{p}p$, $e^+e^- \rightarrow \bar{p}p\gamma$ processes together with angular distributions in $e^-p \rightarrow e^-p$ and $e^+p \rightarrow e^+p$ processes should allow for disentangling of the two-photon exchange contributions from the form factors.

Model testing is simplified if it is implemented into a Monte Carlo event generator. Such a generator serves also for other purposes like calculations of acceptance and/or efficiency corrections. For the radiative return (called also ISR) method such a tool was developed some time ago [11]. Nucleon final states were implemented in it already in [12] and the nucleon form factors were updated in [9], where also the modelling of the final state radiative corrections was addressed. Recently [13] also a possibility of generation of the process $e^+e^- \rightarrow \text{hadrons}$, useful for scan experiments, was added.

Work supported in part by the Polish National Science Centre, grant number DEC-2012/07/B/ST2/03867 and German Research Foundation DFG under Contract No. Collaborative Research Center CRC-1044. Szymon Tracz is supported by the Forszt project co-financed by EU from the European Social Fund.

References

- [1] I. Estermann, R. Frisch, and O. Stern Nature **132** (1933) 169.
- [2] M. N. Rosenbluth, Phys. Rev. **79** (1950) 615.
- [3] R. W. Mcallister and R. Hofstadter, Phys. Rev. **102** (1956) 851.

- [4] R. Hofstadter, Rev. Mod. Phys. **28** (1956) 214.
- [5] J. Arrington, Phys. Rev. C **68** (2003) 034325 [nucl-ex/0305009].
- [6] C. E. Carlson and M. Vanderhaeghen, Ann. Rev. Nucl. Part. Sci. **57** (2007) 171 [hep-ph/0701272 [HEP-PH]].
- [7] C. F. Perdrisat, V. Punjabi and M. Vanderhaeghen, Prog. Part. Nucl. Phys. **59** (2007) 694 [hep-ph/0612014].
- [8] A. Denig and G. Salme, Prog. Part. Nucl. Phys. **68** (2013) 113 [arXiv:1210.4689 [hep-ex]].
- [9] H. Czyz, J. H. Kuhn and S. Tracz, arXiv:1407.7995 [hep-ph].
- [10] G. P. Lepage and S. J. Brodsky, Phys. Rev. D **22** (1980) 2157.
- [11] G. Rodrigo, H. Czyz, J. H. Kuhn and M. Szopa, Eur. Phys. J. C **24** (2002) 71 [hep-ph/0112184].
- [12] H. Czyz, J. H. Kuhn, E. Nowak and G. Rodrigo, Eur. Phys. J. C **35** (2004) 527 [hep-ph/0403062].
- [13] H. Czyz, M. Gunia and J. H. Kuhn, JHEP **1308** (2013) 110 [arXiv:1306.1985, arXiv:1306.1985 [hep-ph]].

2.11 Current status of Monte Carlo generator Tauola

O. Shekhovtsova

Institute of Nuclear Physics PAN, ul. Radzikowskiego 152, 31-342 Krakow, Poland
Kharkov Institute of Physics and Technology, Akademicheskaya,1, 61108 Kharkov, Ukraine

The Monte Carlo generator TAUOLA [1], which is used to simulate tau lepton decays, is a computing project with a rather long history. It started in the years 80's and is under development still now. The main problem in the theoretical description of the hadronic decay modes of the tau lepton is a lack of a theory coming from the first principle in the energy region from the threshold till the tau mass. The hadronic currents in the first version of TAUOLA as well as the subsequent internal versions of the code used by both Aleph and Cleo collaborations were based on the Vector Meson Dominance approach. However, that approach is able to reproduce only the leading-order results of Chiral Perturbation Theory (ChPT). As was shown in the case of the $K^+K^-\pi^-$ mode this approach spoils the Wess-Zumino anomaly normalization, that appears at $O(p^4)$ in ChPT [2]. An alternative approach is to include the lightest resonances as active degrees of freedom in the theory. This can be done by adding resonance fields to the ChPT Lagrangian, without any dynamical assumption, leading to Resonance Chiral Lagrangian approach [3, 4]. The RChL approach succeeds in reproducing low energy results, predicted by ChPT, at least at the next-to-leading order, and also complies with QCD high energy constraints.

Up to now the RChL currents for the main two-meson (final states with two pion, pion-kaon, two kaons) and three-pseudoscalar (three pion, two kaon-one pion) decay modes have been installed into TAUOLA. This set covers more than 88% of the tau lepton hadronic decay width. The implementation of the currents, the related technical tests as well as the necessary theoretical concepts are documented in [5].

To get numerical values of the model parameters one has to fit the theoretically predicted spectra to those measured in experiments. We started with the $\tau^- \rightarrow \pi^- \pi^- \pi^+ \nu_\tau$ decay. The first fit to the preliminary BaBar data [6] allowed to extract numerical values of the model parameters and demonstrated satisfactory agreement with the three pion invariant mass spectrum and a mismatch in the low energy tail of the two pion invariant mass distributions [7]. Improvement has been achieved by adding the σ resonance contribution in the hadronic current [8]. To fit the data we used the MINUIT package through the ROOT framework and the fit result is presented in Fig. 1 of [8]. For the numerical values of the model parameters see Table 1 in [8]. The goodness of the fit is quantified by $\chi^2/\text{ndf} = 6658/401$. To compare with the previous result [7] we have estimated the χ^2 value using the combined statistical and systematic uncertainties and we find $\chi^2/\text{ndf} = 910/401$ that is eight times better than in [7].

The following tests have been done to validate our fitting procedure: asserting statistical errors and correlation coefficients between the model parameters, verifying that the obtained result is a global minimum and performing studies of the systematical errors. A detailed description as well as the results of the tests are presented in [8].

The fitting procedure for the three pion mode has been generalized to an arbitrary three meson final state. Thus the new fitting framework allows to perform fits for arbitrary tau decay mode, using either Fortran or C++ code. To test it, we have first reproduced the results for the three pion decay mode described above and then fitted the $K^+K^-\pi^-$ currents to the BaBar preliminary data [6]. For the moment we have used some simplifications for the $K^+K^-\pi^-$ current which will be removed in the final version of the fitting strategy. In addition, fits for $\tau^- \rightarrow \pi^-\pi^0\nu_\tau$ decay mode has been added allowing to fit the RChL two pion form factor to the Belle parameterization. Next step will be to study the stability of the generalized fitting procedure and to include the experimental errors.

Another important task concerned the C++ interface for the decay channels of TAUOLA generator. The interface allows to add, substitute or modify TAUOLA decay modes using either C++ or FORTRAN code. The interface is ready to be used in Tauola++ project (<http://tauolapp.web.cern.ch/tauolapp/>) as well as in the FORTRAN environments, where TAUOLA is still being used. Validation of all BaBar currents introduced along with the C++ environment has been finished and extensive testing of the environment has been performed.

This research was supported in part by Foundation of Polish Science grant POMOST/2013-7/12, that is co-financed from European Union, Regional Development Fund and from funds of Polish National Science Centre under decisions DEC-2011/03/B/ST2/00107.

References

- [1] S. Jadach, Z. Was, R. Decker and J. H. Kuhn, Comput. Phys. Commun. **76** (1993) 361.
- [2] T. E. Coan *et al.* [CLEO Collaboration], Phys. Rev. Lett. **92** (2004) 232001 [hep-ex/0401005].
- [3] G. Ecker, J. Gasser, A. Pich and E. de Rafael, Nucl. Phys. B **321** (1989) 311.
- [4] G. Ecker, J. Gasser, H. Leutwyler, A. Pich and E. de Rafael, Phys. Lett. B **223** (1989) 425.
- [5] O. Shekhovtsova, T. Przedzinski, P. Roig and Z. Was, Phys. Rev. D **86** (2012) 113008 [arXiv:1203.3955 [hep-ph]].
- [6] I. M. Nugent, T. Przedzinski, P. Roig, O. Shekhovtsova and Z. Was, Phys. Rev. D **88** (2013) 9, 093012 [arXiv:1310.1053 [hep-ph]].
- [7] O. Shekhovtsova, I. M. Nugent, T. Przedzinski, P. Roig and Z. Was, arXiv:1301.1964 [hep-ph].
- [8] I. M. Nugent, arXiv:1301.7105 [hep-ex].

3 List of participants

- Antonio Anastasi, University of Messina and LNF, antonioanastasi89@gmail.com
- Marcin Berłowski, National Center for Nuclear Research, Marcin.Berłowski@fuw.edu.pl
- Bo Cao, University of Uppsala, bo.cao@physics.uu.se
- Carlo M. Carloni Calame, University of Pavia, carlo.carloni.calame@pv.infn.it
- Henryk Czyż, University of Silesia, henryk.czyz@us.edu.pl
- Achim Denig, Universität Mainz, denig@kph.uni-mainz.de
- Gennadiy V. Fedotov, BINP and NSU, G.V.Fedotov@inp.nsk.su
- Martin Hoferichter, University of Bern, hoferichter@itp.unibe.ch
- Karol Kołodziej, University of Silesia, karol.kolodziej@us.edu.pl
- Andrzej Kupsc, University of Uppsala, Andrzej.Kupsc@physics.uu.se
- Peter Lukin, BINP and NSU, P.A.Lukin@inp.nsk.su
- Pere Masjuan, Universität Mainz, masjuan@kph.uni-mainz.de
- Dario Moricciani, INFN - Roma Tor Vergata, moricciani@roma2.infn.it
- Massimo Passera, INFN Padova, passera@pd.infn.it
- Olga Shekhovtsova, IFJ PAN, Olga.Shekhovtsova@lnf.infn.it
- Szymon Tracz, University of Silesia, szymon885@gazeta.pl
- Graziano Venanzoni, LNF, Graziano.Venanzoni@lnf.infn.it
- Ping Wang, Institute of High-energy Physics, Beijing, wangp@ihep.ac.cn